Estimate of gas transfer velocity in the presence of emergent vegetation using argon as a tracer: implications for whole-system denitrification measurements

Elisa Soana[#], Elisa Anna Fano, Giuseppe Castaldelli

Department of Life Sciences and Biotechnology, University of Ferrara, Via L. Borsari 46 – 44121 Ferrara – Italy

[#] Corresponding author: elisa.soana@unife.it

Abstract

Denitrification associated with emergent macrophytes is a pivotal process underlying the treatment performance of wetlands and slow-flow waterways. Laboratory scale experiments targeting N losses via denitrification in sediments colonized by emergent macrophytes require the use of mesocosms that are necessarily open to the atmosphere. Thus, the proper quantification of N_2 effluxes relies on the accurate characterization of the air–water gas exchanges. In this study, we present a simple approach for direct measurements of the gas transfer velocity, in open-top mesocosms with *Phragmites australis*, by using argon as a tracer. Different conditions of water velocity (0, 1.5, 3, and 6 cm s^{-1}) and temperature (8.5, 16, and 28 °C), were tested, along with, for the first time, the presence of emergent vegetation. The outcomes demonstrated that water velocity and temperature are not the only factors regulating aeration at the mesocosm scale. Indeed, the gas transfer velocity was systematically higher, in the range of 42−53%, in vegetated compared to unvegetated sediments. The increase of small-local turbulence patterns created within water parcels moving around plant stems translated into significant modifications of the reaeration process. The adopted approach may be used to improve the accuracy of denitrification measurements by N_2 efflux-based methods in wetland and slow-flow waterway sediments colonized by emergent macrophytes. Moreover, the present outcomes may have multiple implications for whole-system metabolism estimations from which largely depend our understanding of biogeochemical dynamics in inland waters that have strong connections to worldwide issues, such as nitrate contamination and greenhouse gas emissions.

Keywords

Air–water gas exchange; argon; emergent vegetation; water velocity; wetlands; denitrification

1. Introduction

Emergent vegetation is a key component of wetland ecosystems, deeply affecting deeply their treatment performances, especially with respect to reactive nitrogen (N), and contributing to eutrophication control (Brisson and Chazarenc, 2009; Faulwetter et al., 2009). This relevant ecosystem service is supported by the coupling of organic N mineralization, nitrification, and denitrification, occurring where the synergic metabolism of plants and bacteria results in the establishment of proximate oxic and anoxic micro-niches, e.g., in the rhizosphere and in periphytic mats (Zhang et al., 2016; Hines, 2006). Experimental micro and mesocosms are diffusely used as robust models to investigate the processes underlying wetland treatment performance. This approach can mimic aspects of the environmental complexity of full-scale systems, while maintaining the ability to control for certain elements such as plant type, hydraulic conditions and nutrient concentrations, and allowing adequate replications to strengthen statistical confidence in comparisons among treatments (Zhang et al., 2008; Maltais-Landry et al 2009a; Moore et al., 2016; Liang et al., 2017). Laboratory scale experiments, performed using micro or mesocosms to incubate emergent wetland vegetation, are necessarily open to the atmosphere. Due to the impossibility of closing the cores and isolating the water from the atmosphere, the presence of emergent plants complicates the experimental set-up and makes standard protocols for measuring gas fluxes from sediments with microphytobenthos or submerged macrophytes unapplicable (Dalsgaard et al., 2000; Racchetti et al., 2017). Emissions of biological trace gasses such as nitrous oxide and methane are thus usually carried out with static chambers that include the three compartments, i.e. sediment, water, and atmosphe (Cheng et al., 2007; de Klein and van der Werf, 2014). The same approach becomes challenging when measuring denitrification by directly quantifying its end-product (N_2) production due to the need to evaluate small changes in concentrations against the elevated atmospheric background (Groffman et al., 2006). Therefore, the denitrification potential of natural, restored or constructed wetlands has been evaluated mainly by the only disappearance of the process substrate, i.e., nitrate (NO_3^-) in water (Brisson and Chazarenc, 2009; Maltais-Landry et al., 2009b; de Klein and van der Werf, 2014), while

fewer studies have simultaneously measured NO_3^- consumption and N_2 production and proved that the removed N is actually lost from the system after conversion to N_2 (Jacobs and Harrison, 2014; Payne et al., 2014; Messer et al., 2017). Highlighting the relative importance of permanent NO_3^- dissipation over other temporary storage mechanisms is crucial to evaluate wetland performance and to adopt management strategies aimed at optimizing their nutrient removal efficiency. For the same reason, denitrification rates representative of *in situ* conditions are needed rather than potential activity assays that eliminate the structural integrity of sediment with associated biogeochemical gradients and the direct influence of plants (Groffman et al., 2006; Xu et al., 2013; Álvarez-Rogel et al., 2016).

At the scale of both mesocosms and whole systems, denitrification can be estimated by directly measuring N_2 accumulation in the water over time, which is possible using high-precision Membrane Inlet Mass Spectrometry (MIMS, Kana et al., 1994), but necessarily taking into account the gas exchanges between water and atmosphere, on which the accuracy of the outcomes largely depends (Castaldelli et al., 2015; Messer et al., 2017). For mesocosms, the parameter describing the molecular diffusivity of a gas across the air–water interface, i.e. the gas transfer velocity (k), is frequently estimated by empirical models as a function of wind speed, the most important variable affecting the stirring force in lentic systems (e.g., Maltais-Landry et al 2009a; Christensen et al., 2013). However, the relationship between k and wind speed typically breaks down under low wind conditions, and in any event, this approach is not applicable for indoor greenhouse experiments. Mesocosms can also simulate the condition of slow-flow waterways or wetlands where gas exchanges across the air-water interface are affected by the turbulence induced by moving water (Audet et al., 2017; Messer et al., 2017). Moreover, the presence of emergent vegetation contributes to modify the common drivers of gas transfer at a small-scale, e.g., by attenuating wind speed above the water surface and affecting hydraulic parameters related to mixing and turbulence (Naden et al., 2006; Coates and Folkard, 2009; Poindexter and Variano, 2013).

Predicting k values that accurately describe the air-water gas exchanges remains a critical challenge for reliable estimations of aquatic ecosystem metabolism, with relevant implications for understanding some biogeochemical dynamics that have strong connections to worldwide issues such as NO_3^- contamination and greenhouse gas emissions. In this study, we present a simple approach for direct measurements of k, in open-top wetland mesocosms with emergent macrophytes, by using argon (Ar) as a tracer. The gas transfer velocity was calculated by the decrease of the Ar concentration in mesocosms incubated in controlled conditions. We preferred to use mesocosms that mimic field conditions in order to be able to standardize and isolate crucial parameters affecting the air-water gas exchange, such as temperature and water velocity, tested for the first time in the presence or absence of emergent vegetation.

2. Material and methods

2.1. Mesocosm construction and pre-incubation procedure

Water, sediments colonized by *Phragmites australis* (Cav.) Trin. ex Steud and bare sediments were collected in early spring in a slow-flow (< 10 cm s^{-1}) nutrient-rich drainage canal (44°48'53.17''N; 11°43'23.14''E) that belongs to the drainage network of the lower Po plain (Northern Italy). Experiments were then performed after the plants had reached the biomass peak. The mesocosms were designed to simulate low-gradient shallow waterways or wetlands with moving water and consisted of two Plexiglass liners (diameter of 12 and 29 cm) positioned concentrically on a flat base. Only the volume between the two liners was filled with a sediment layer of 25−30 cm to define an annulus of total surface of 547 cm^2 (annular radius width 8.5 cm). Three mesocosms with sediment and *P. australis* (1200−1900 plants per m^2, stem average diameter 4 mm) and three mesocosms with only sediment were built and transferred to an outdoor, non-shaded area, at the Department of Life Sciences and Biotechnology, University of Ferrara. Here, the mesocosms were placed in a cylindrical tank, fully submerged in recirculated canal water maintained by aquarium pumps and were allowed to equilibrate for some weeks before the experiments. Sampling, pre-incubation and incubation

procedures were performed according to standard protocols (Dalsgaard et al., 2000). The same experimental set up was previously employed to investigate how different water velocity conditions affect NO_3^- removal via denitrification in sediments with emergent vegetation (Soana et al., 2018; Castaldelli et al., 2018).

2.2. Ar gas tracer addition experiments

The first set of four incubations (*velocity experiment*) was performed, at a fixed temperature (16 °C), to test how *P. australis* affects gas exchange at different water velocities (0, 1.5, 3 and 6 cm s^{-1}) in the range typical of wetlands and slow-flow canals. The second set of three incubations (*temperature experiment*) was performed, at a fixed water velocity (3 cm s^{-1}), to test how *P. australis* affects gas exchange at different water temperatures (8.5 °C, 16 °C, and 28 °C), spanning the typical seasonal range for shallow aquatic ecosystems of temperate regions (Racchetti et al., 2011; Castaldelli et al., 2015).

A perforated plastic tube jointed to a 12 V submersible electric pump (Whale®, Bangor, UK) was placed vertically in the water column of each mesocosm. The pump was connected to a multichannel electronic rheostat and a voltage was applied to create a homogeneous water flow around the internal Plexiglass liner avoiding sediment resuspension and waves at the water surface. The voltage level was regulated to yield an average water velocity of 0, 1.5, 3, and 6 cm s^{-1}, checked vertically in the middle of the annular radius and at mid-depth by means of a current meter. All experiments were performed in the dark and a thermostat ensured the stability of the water temperature through the course of each incubation. Wind speed was null during the experiments.

To begin the incubations, the water level in the tank was lowered below the liner top and a water column of ~ 20 cm was maintained inside each mesocosm. Argon, an inert tracer gas, was bubbled for ~ 10 min at 10 psi from a compressed Ar tank (SOL SpA, Bologna, Italy) using a gas diffuser to saturate the water volume of each mesocosm. Once the gas sparging was stopped, water samples were collected at 30-minute interval over a 4.5-h period by a glass gas-tight syringe from the mid-depth of

each mesocosm in order to follow the temporal evolution of Ar in water. At each sampling event, the water temperature and conductivity were measured with a multiparametric probe. Samples for dissolved Ar determinations were collected with no headspace in 12-mL gas-tight glass vials (Exetainer®, Labco, High Wycombe, UK), filled from the bottom by overflowing the vial volume at least 3 times, and preserved by adding 100 µL of saturated $ZnCl_2$ solution. Ar was measured within a few days at the laboratory of Aquatic Ecology, University of Ferrara, by MIMS (Bay Instruments, Easton, Maryland, USA), a PrismaPlus quadrupole mass spectrometer with an inline furnace operating at 600°C to allow for O_2 removal (Kana et al., 1994). The coefficient of variation (cv) of mass spectrometry signal (m/z = 40) for replicated samples was < 0.5%.

2.3. Calculation of gas transfer velocity from Ar addition experiments

Due to its conservative behavior, the dissolved Ar concentration was assumed to decrease only as a consequence of gas escape to the atmosphere. The gas transfer velocity was calculated following the procedure reported by Czerny et al. (2013) and previously applied for other tracer gases. Negative exponential functions were fitted to the series describing the temporal evolution of Ar in the water volume of each mesocosm for each tested condition. A correction factor was introduced in the calculations to account for the water volume loss from the subsequent samplings, although the total volume collected for Ar analysis during the course of a single incubation was overall < 3% of the volume of each mesocosm. For vegetated mesocosms, the volume occupied by the submerged portions of the plants was also considered by measuring the diameters of each reed stem. Pilot tests performed with the simultaneous addition of Ar and a solute tracer revealed that volume loss due to evapotranspiration was irrelevant on the incubation time scale of a few hours and that, once the mesocosms were isolated from each other by lowering the water level in the tank, there was no water exchange between the chambers and the tank.

166 The hourly Ar flux across the water surface (µmol cm^{-2} h^{-1}) was calculated from the fitted Ar
167 concentration decrease between two consecutive sampling times, then converted to volumetric units
168 according to the following equation:

169 $$F_{Ar} = \frac{I_{t2} - I_{t1}}{A \cdot \Delta t} \quad (1)$$

170 where I_{t1} and I_{t2} are the µmol of Ar in the mesocosm water volume at two consecutive sampling times,
171 t_1 and t_2, A is the surface area of the mesocosm (cm^2), and Δt is the time interval between t_1 and t_2
172 (h). The Ar transfer velocity (cm h^{-1}) was computed by dividing the F_{Ar} by the concentration gradient
173 according to the following equation:

174 $$k_{Ar} = \frac{F_{Ar}}{C_{ArW} - C_{ArEW}} \quad (2)$$

175 where F_{Ar} is the Ar flux across the water surface, and C_{ArW} is the fitted Ar concentration (µmol cm^{-2}
176 h^{-1}) at a given sampling time, and C_{ArEW} is the Ar equilibrium concentration with the atmosphere
177 (µmol cm^{-3}) determined from tables of gas solubility in water as a function of temperature and
178 conductivity (Weiss, 1970). The two previous equations were applied to all the couples of two
179 consecutive sampling events throughout the whole incubation time, and finally, k_{Ar} for each
180 mesocosm in each tested condition was calculated as general mean.
181 The Ar transfer velocity was corrected for temperature effect, according to the generally used
182 simplified Arrhenius equation (Demars and Manson, 2013):

183 $$k_{Ar} = k_{Ar20°C} \cdot 1.0241^{(T-20°C)} \quad (3)$$

184 where k_{Ar} and $k_{Ar20°C}$ are the Ar transfer velocities at the measured water temperature (T, °C) and at
185 20 °C, respectively. As usual for comparison purposes, the gas transfer velocity was expressed for a
186 gas with a Schmidt number of 600 (k_{600}) which corresponds to CO_2 at 20 °C (Jähne et al., 1987;
187 Wanninkhof, 1992) as follows:

188 $$k_{600} = k_{Ar20°C} \cdot \left(\frac{Sc_{CO_2}}{Sc_{Ar}}\right)^{-2/3} \quad (4)$$

189 where $k_{Ar20°C}$ is the Ar transfer velocity at 20°C, Sc_{CO_2} and Sc_{Ar} are the Schmidt number for CO_2
190 (600) and Ar (518) at 20°C, respectively.

A one-way ANOVA was performed to analyze differences in k values among the tested conditions. Untransformed data satisfied assumptions of normality. The statistical significance was set at $p < 0.05$. Statistical analyses were performed with SigmaPlot 11.0 (Systat Software, Inc., San Jose, California, USA).

2.4. Calculation of the gas transfer velocity by empirical equations from the literature

Excluding the conditions with no flow, the reaeration coefficient of oxygen at 20 °C (KO_2, 20 °C, d^{-1}) was also calculated using the water velocity *u* (m s^{-1}) and water depth *d* (m) of the mesocosms as the only variables affecting gas exchanges, by the general relationship (Genereux and Hemond, 1992):

$$K_{O_2} = a \cdot \frac{u^b}{d^c} \quad (5)$$

The parameters of *a*, *b*, and *c* were obtained from several literature studies as compiled by Haider et al. (2013). These equations have been tested and applied in laminar flow channels, artificial flumes, and regular-shaped sewers where flow conditions approximate those set in our mesocosms (Cox, 2003). The transfer velocity of oxygen (kO_2, 20 °C, cm h^{-1}) was obtained by multiplying the reaeration coefficient by the water column depth of each mesocosm, assuming a well-mixed conditions. The gas transfer velocity was finally normalized to a Schmidt number of 600 according to equation 4.

3. Results

Changes in Ar concentrations in the water column of the mesocosms during the experiments are presented in Fig. 1. Ar concentrations, expressed as a natural-log transformed proportion of initial value, decreased steadily throughout the course of incubations, suggesting constant gas escape to the atmosphere from all mesocosms. The slopes of the time series were all highly significant ($p < 0.0001$) and had R^2 values that ranged from 0.88 to 0.99. Across the velocity range, k_{Ar} ranged between 0.678 ± 0.129 and 5.452 ± 0.589 cm h^{-1} in vegetated mesocosms, and between 0.669 ± 0.128 and 3.586 ±

0.353 cm h^{-1} in unvegetated mesocosms (Table 1). The gas transfer velocity differed significantly among all velocity treatments ($p < 0.001$) and was increased on average by a factor of 8 and 5 in vegetated and unvegetated sediments, respectively, when passing from the stagnant condition to 6 cm s^{-1}. With the exception of stagnant conditions where k_{Ar} was not significantly different between vegetated and unvegetated mesocosms, for the other velocity levels, the presence of the macrophytes strongly influenced k_{Ar} ($p < 0.001$). The gas transfer velocity was systematically higher, in the range 42−53%, in the presence of emergent vegetation.

Throughout the water temperature range, k_{Ar} varied between 3.938 ± 0.277 and 6.458 ± 0.325 cm h^{-1} and between 2.463 ± 0.128 and 4.255 ± 0.236 cm h^{-1} in vegetated and unvegetated mesocosms, respectively (Table 1). The gas exchange was enhanced on average by ~ 40% when the water temperature changed from 8.5 °C to 28 °C, and k_{Ar} was significantly higher for the vegetated condition. Once transformed as k_{600} at 20 °C, experimental k_{Ar} values measured at different temperatures were not significantly different, although the discrepancy between vegetated and unvegetated conditions remained.

k_{600} values measured in mesocosms were included within the interquartile range of the distribution obtained by applying empirical equations from the literature but were systematically higher than the median value, i.e., by a factor of 1.9−3.7 and 1.3−2.6 for vegetated and unvegetated conditions, respectively (Fig. 2).

4. Discussion

The results presented here have two main methodological implications: 1) the possibility to operate a direct quantification of the gas transfer velocity in open-top wetland mesocosms, in conditions of variable water velocity and temperature and, 2) the assessment of the role of emergent vegetation in affecting reaeration processes with potential consequences for whole-system metabolism measurements involving gas dynamics, as N_2 production by denitrification. The outcomes of our incubations proved the reliability of the proposed approach, i.e., the absence of other unpredictable

242 factors affecting the gas air-water exchanges (apart from water velocity and plant presence) since
243 there were no significant differences between the k_{Ar} measured at different temperatures, once
244 transformed to k_{600} at 20 °C. Tracer gas addition is a common effective means of directly measuring
245 reaeration in different types of aquatic ecosystems (i.e. stream, lakes) (Cole et al., 2010; Demars et
246 al., 2015). Other inert gases such as sulfur hexafluoride (SF_6) were previously used as tracers to
247 quantify gas exchange rate also at the mesocosm scale, but only for free-water conditions (Langdon
248 et al., 2003) or in presence of floating vegetation (Jacobs and Harrison, 2014). With respect to
249 emergent vegetation, we found only one study where, in the framework of a ^{15}N mass balance, the
250 gas transfer velocity has been measured by quantifying Ar degassing after addition to the water
251 column (Messer et al., 2017). Hall and Madinger (2018) recently recommended the use of Ar because
252 it has low background concentrations in water and, unlike other gases commonly used as tracers, it is
253 cheaply available and is not a greenhouse gas, such as SF_6. Moreover, Ar is easily detected using
254 MIMS which has become in the last twenty years a standard instrument for biogeochemical studies
255 targeting aquatic metabolism. Indeed, it allows the simultaneous measurement of several gases of
256 biological interest, such as N_2 isotopes (28, 29, 30), O_2, and CH_4 with high analytical precision (Kana
257 at al., 1994; Schrier-Uijl et al., 2011; Soana et al., 2017).
258 To our knowledge, prior than this study, no experiments are available in the literature on the
259 comparison of gas transfer across the air-water interface in sediments with and without emergent
260 plants. Moreover, it is not clear if the models commonly used for the estimations of gas transfer
261 velocity in aquatic environments, as a function of hydraulic parameters affecting turbulence and
262 mixing (e.g. velocity and depths), can be directly applied to sediment with emergent vegetation
263 (Naden et al., 2006; Coates and Folkard, 2009). In field studies suggest that no universally acceptable
264 predictive model was found for the k estimation on the basis of the sole hydraulic properties in
265 shallow macrophyte-rich watercourses (Thyssen et al., 1987; Wilcock et al., 1999). Indeed, none
266 empirical equation includes parameters related to vegetation stand features (e.g., typology, flexibility,
267 density, arrangement, patchiness etc.) due to the evident difficulty in describing the great spatial and

temporal heterogeneity and complexity of *in situ* conditions. The outcomes of the present experiment clearly demonstrated, for the first time, that emergent macrophytes noticeably increase gas exchanges across the air-water interface. Aquatic vegetation with partially or totally submerged tissues complicate the dependency of the gas exchange on velocity and depth by directly affecting parameters related to turbulence and mixing (Nepf, 1999; Nikora, 2010). In general, water has a more tortuous flow path while moving around the plant stems, resulting in an increase of small-scale turbulence. Submerged or emergent macrophytes promote several mechanisms of turbulence generation (e.g., vortex shedding along shear zones, wake production around individual stems, waving of flexible plant forms), thus modifying local patterns of turbulence intensities that greatly differ from those found in unvegetated flows (Naden et al., 2006; Tanino, 2012). The variability of k_{600} values within replicates was generally greater for vegetated mesocosms than for unvegetated mesocosms. This is likely due to the greater environmental heterogeneity in the vegetated mesocosms, determined by the variable number of stems. Despite the limited number of replicates, for all the performed incubations the gas transfer velocity resulted positively related to stem density, with R^2 values ranging from 0.90 to 0.98. We are aware that these results are preliminary and need further and more detailed (i.e., wider stem density range and more replicates for a given vegetation density) measurements. However, fluid dynamic studies have previously demonstrated that an increase in density of rigid vegetation translates proportionally into an enhancement of turbulence by introducing additional hydraulic resistance to flow (Yager and Schmeeckle, 2013; Horppila et al., 2013). The turbulence created within a water parcel moving around the stems acts to break the resistance of the aqueous boundary layer, facilitating the gas exchanges across the air-water interface (Naden et al., 2006; Tanino, 2012).

Several laboratory experiments, mainly involving artificial plants, have investigated many aspects of water flow dynamics within vegetation stands and their effect in modifying small-scale turbulence (Yager and Schmeeckle, 2013; Zhang et al., 2015). However, they were performed almost exclusively to describe the physics of the system without extending the results to the potential ecological implications in terms of aquatic metabolism estimations. Air-water gas exchange is a key process in

aquatic ecosystems because its quantification allows distinguishing between physical and biologically-mediated gas fluxes. Obtaining a proper estimate of reaeration rate is the most critical step when calculating metabolism in open systems, from the classical Odum oxygen approach to the more innovative N_2 open-channel approach (Demars et al., 2015; Soana et al., 2017; Ritz et al., 2018). When direct measurements of gas transfer velocity are not available, a conservative approach generally results the most reasonable option, i.e., the adoption of a wide set of depth-velocity equations with the aim of providing a range of k_{600}, likely including the actual value. With respect to N dynamics, this procedure is widespread for both whole-system (Castaldelli et al., 2015; Ritz et al., 2018) and mesocosm scale estimates of denitrification (Soana et al., 2018; Castaldelli et al., 2018). However, the considerable variability in gas exchange rates may undermine the estimates of ecosystem metabolism, e.g., NO_3^- removal via denitrification, based on such equations and bias the interpretation. Moreover, the present outcomes clearly showed that, for a given water velocity, increased small-scale turbulence resulted in higher k_{600} values in vegetated mesocosms with respect to unvegetated mesocosms. Although our experimental k_{600} values were included within the confidence interval of those calculated using empirical equations, the systematic difference between vegetated and unvegetated conditions raises some doubts about the validity of using literature-derived formulas to predict reaeration in flowing waters with emergent macrophytes. The magnitude of reaeration is directly related to the uncertainty in estimates of metabolic rates. Specifically, given the linear form of the equations governing the biogenic gas mass balance in water, under or overestimates of gas transfer velocity translate proportionately into under or overestimates of gas production or consumption, respectively. With respect to N dynamics, underestimates of k_{600} of up to ~ 50%, as evidenced in this study, translate proportionately into underestimates of the NO_3^- mitigation potential of vegetated sediments.

In conclusion, the approach presented here may be used to improve the accuracy of aquatic metabolism estimates in open-systems, such as denitrification measurements by N_2 efflux-based methods, in slow-flow waterways and wetland sediments colonized by emergent macrophytes. Site-

specific or mesocosm-specific measurements of gas transfer velocity are indispensable since variables such as abundance/density, development and geometric and mechanical properties of vegetation stands may influence, differently from case to case, the local turbulence patterns thus also the gas exchanges across the air-water interface.

Acknowledgements

This work was financially supported by the Emilia-Romagna Region within the Rural Development Programme (PSR) 2014–2020 (Measure 16.1.01 - Operational Groups of the European Partnership for Agricultural Productivity and Sustainability) and within the POR FESR 2007–2013 Programme (Industrial Research and Technology Transfer) for the development of the Regional High Technology Network. It was also supported by the Po Delta Regional Park of the Emilia-Romagna within a long-term research collaboration aiming at defining management protocols for the control of eutrophication in the Po River Delta. The authors would like to thank Anna Gavioli and Fabio Vincenzi for their help during sampling and laboratory activities.

References

Álvarez-Rogel, J., del Carmen Tercero, M., Arce, M.I., Delgado, M.J., Conesa, H.M., González-Alcaraz, M.N., 2016. Nitrate removal and potential soil N_2O emissions in eutrophic salt marshes with and without *Phragmites australis*. Geoderma 282, 49–58.

Audet, J., Neif, É.M., Cao, Y., Hoffmann, C.C., Lauridsen, T.L., Larsen, S.E., Søndergaard, M., Jeppesen, E., Davidson, T.A., 2017. Heat-wave effects on greenhouse gas emissions from shallow lake mesocosms. Freshw. Biol. 62(7), 1130–1142.

Brisson, J., Chazarenc, F., 2009. Maximizing pollutant removal in constructed wetlands: should we pay more attention to macrophyte species selection? Sci. Total Environ. 407(13), 3923–3930.

Castaldelli, G., Soana, E., Racchetti, E., Vincenzi, F., Fano, E.A., Bartoli, M., 2015. Vegetated canals mitigate nitrogen surplus in agricultural watersheds. Agr. Ecosyst. Environ. 212, 253–262.

Castaldelli, G., Aschonitis, V., Vincenzi, F., Fano, E.A., Soana, E., 2018. The effect of water velocity on nitrate removal in vegetated waterways. J. Environ. Manage. 215, 230–238.

Cheng, X., Peng, R., Chen, J., Luo, Y., Zhang, Q., An, S., Chen, J., Li, B., 2007. CH_4 and N_2O emissions from *Spartina alterniflora* and *Phragmites australis* in experimental mesocosms. Chemosphere 68(3), 420–427.

Christensen, J., Sand-Jensen, K., Staehr, P.A., 2013. Fluctuating water levels control water chemistry and metabolism of a charophyte-dominated pond. Freshw. Biol. 58(7), 1353–1365.

Coates, M.J., Folkard, A.M. 2009. The effects of littoral zone vegetation on turbulent mixing in lakes. Ecol. Model. 220, 2714–2726.

Cole, J.J., Bade, D.L., Bastviken, D., Pace, M.L., Van de Bogert, M., 2010. Multiple approaches to estimating air-water gas exchange in small lakes. Limnol. Oceanogr.-Meth. 8(6), 285–293.

Cox, B.A., 2003. A review of dissolved oxygen modelling techniques for lowland rivers. Sci. Total Environ. 314, 303–334.

Czerny, J., Schulz, K.G., Ludwig, A., Riebesell, U., 2013. Technical Note: A simple method for air–sea gas exchange measurements in mesocosms and its application in carbon budgeting. Biogeosciences, 10(3), 1379–1390.

Dalsgaard, T., Nielsen, L.P., Brotas, V., Viaroli, P., Underwood, G.J.C., Nedwell, D.B., Sundbäck, K., Rysgaard, S., Miles, A., Bartoli, M., Dong, L., Thornton, D.C.O., Ottosen, L.D.M., Castaldelli, G., Risgaard-Petersen, N., 2000. Protocol Handbook for NICE-Nitrogen Cycling in Estuaries: A Project Under the EU Research Programme. Marine Science and Technology (MAST III). National Environmental Research Institute, Silkeborg, Denmark, 62 pp.

de Klein, J.J., van der Werf, A.K., 2014. Balancing carbon sequestration and GHG emissions in a constructed wetland. Ecol. Eng. 66, 36–42.

Demars, B.O.L., Manson, J.R., 2013. Temperature dependence of stream aeration coefficients and the effect of water turbulence: a critical review. Water Res. 47(1), 1–15.

Demars, B.O., Thompson, J., Manson, J.R., 2015. Stream metabolism and the open diel oxygen method: Principles, practice, and perspectives. Limnol. Oceanogr.-Meth. 13(7), 356–374.

Faulwetter, J.L., Gagnon, V., Sundberg, C., Chazarenc, F., Burr, M.D., Brisson, J., Camper, A.K., Stein, O.R., 2009. Microbial processes influencing performance of treatment wetlands: a review. Ecol. Eng. 35(6), 987–1004.

376 Genereux D.P., Hemond H.F., 1992. Gas exchange rate constant for a small stream on Walker Branch
377 watershed, Tennessee. Water Resour. Res. 28, 2365–2374.

378 Groffman, P.M., Altabet, M.A., Böhlke, J.K., Butterbach-Bahl, K., David, M.B., Firestone, M.K.,
379 Giblin, A.E., Kana, T.M., Nielsen, L.P., Voytek, M.A., 2006. Methods for measuring denitrification:
380 diverse approaches to a difficult problem. Ecol. Appl. 16(6), 2091–2122.

381 Haider, H., Ali, W., Haydar, S., 2013. Evaluation of various relationships of reaeration rate coefficient
382 for modeling dissolved oxygen in a river with extreme flow variations in Pakistan. Hydrol. Process.
383 27, 3949–3963.

384 Hall, R.O. Jr, Madinger, H.L., 2018. Use of argon to measure gas exchange in turbulent mountain
385 streams. Biogeosciences 15(10), 3085–3092.

386 Hines, M.E., 2006. Microbially mediated redox cycling at the oxic–anoxic boundary in sediments:
387 comparison of animal and plants habitats. Water Air Soil Poll. 6(5-6), 523–536.

388 Horppila, J., Kaitaranta, J., Joensuu, L., Nurminen, L., 2013. Influence of emergent macrophyte
389 (*Phragmites australis*) density on water turbulence and erosion of organic-rich sediment. J.
390 Hydrodyn. 25(2), 288–293.

391 Jähne, B., Munnich, K.O., Bosinger, R., Dutzi, A., Huber, W., Libner, P., 1987. On parameters
392 influencing air–water exchange. J.Geophys. Res. 1937–1949.

393 Kana, T.M., Darkangelo, C., Hunt, M.D., Oldham, J.B., Bennett, G.E., Cornwell, J.C., 1994.
394 Membrane inlet mass spectrometer for rapid high-precision determination of N_2, O_2, and Ar in
395 environmental water samples. Anal. Chem. 66(23), 4166–4170.

396 Langdon, C., Broecker, W.S., Hammond, D.E., Glenn, E., Fitzsimmons, K., Nelson, S.G., Peng, T.H.,
397 Hajdas, I., Bonani, G., 2003. Effect of elevated CO_2 on the community metabolism of an experimental
398 coral reef. Global Biogeochem. Cy. 17(1).

399 Liang, Y., Zhu, H., Bañuelos, G., Yan, B., Shutes, B., Cheng, X., Chen, X., 2017. Removal of
400 nutrients in saline wastewater using constructed wetlands: plant species, influent loads and salinity
401 levels as influencing factors. Chemosphere 187, 52–61.

402 Maltais-Landry, G., Maranger, R., Brisson, J., 2009a. Effect of artificial aeration and macrophyte
403 species on nitrogen cycling and gas flux in constructed wetlands. Ecol. Eng. 35(2), 221–229.

404 Maltais-Landry, G., Maranger, R., Brisson, J., Chazarenc, F., 2009b. Nitrogen transformations and
405 retention in planted and artificially aerated constructed wetlands. Water Res. 43(2), 535–545.

406 Messer, T.L., Burchell, M.R., Böhlke, J.K., Tobias, C.R., 2017. Tracking the fate of nitrate through
407 pulse-flow wetlands: A mesocosm scale ^{15}N enrichment tracer study. Ecol. Eng. 106, 597–608.

408 Moore, M.T., Locke, M.A., Kröger, R., 2016. Using aquatic vegetation to remediate nitrate,
409 ammonium, and soluble reactive phosphorus in simulated runoff. Chemosphere 160, 149–154.

410 Naden, P., Rameshwaran, P., Mountford, O., Robertson, C., 2006. The influence of macrophyte
411 growth, typical of eutrophic conditions, on river flow velocities and turbulence production. Hydrol.
412 Process. 20(18), 3915–3938.

413 Nepf, H.M., 1999. Drag, turbulence, and diffusion in flow through emergent vegetation. Water
414 Resour. Res. 35(2), 479–489.

415 Nikora, V., 2010. Hydrodynamics of aquatic ecosystems: an interface between ecology,
416 biomechanics and environmental fluid mechanics. River Res. Appl. 26(4), 367–384.

417 Payne, E. G., Fletcher, T.D., Russell, D.G., Grace, M.R., Cavagnaro, T. R., Evrard, V., Deletic, A.,
418 Hatt, B.E., Cook, P.L., 2014. Temporary storage or permanent removal? The division of nitrogen
419 between biotic assimilation and denitrification in stormwater biofiltration systems. PloS One 9(3),
420 e90890.

421 Poindexter, C.M., Variano, E.A., 2013. Gas exchange in wetlands with emergent vegetation: The
422 effects of wind and thermal convection at the air-water interface. J. Geophys. Res.-Biogeosci. 118(3),
423 1297–1306.

424 Racchetti, E., Bartoli, M., Soana, E., Longhi, D., Christian, R.R., Pinardi, M., Viaroli, P., 2011.
425 Influence of hydrological connectivity of riverine wetlands on nitrogen removal via denitrification.
426 Biogeochemistry 103(1-3), 335–354.

427 Racchetti, E., Longhi, D., Ribaudo, C., Soana, E., Bartoli, M., 2017. Nitrogen uptake and coupled
428 nitrification–denitrification in riverine sediments with benthic microalgae and rooted macrophytes.
429 Aquatic Sci. 79(3), 487–505.

430 Ritz, S., Dähnke, K., Fischer, H., 2018. Open-channel measurement of denitrification in a large
431 lowland river. Aquatic Sci. 80(1), 11.

432 Schrier-Uijl, A.P., Veraart, A.J., Leffelaar, P.A., Berendse, F., Veenendaal, E.M., 2011. Release of
433 CO 2 and CH 4 from lakes and drainage ditches in temperate wetlands. Biogeochemistry 102(1–3),
434 265–279.

435 Soana, E., Balestrini, R., Vincenzi, F., Bartoli, M., Castaldelli, G. (2017). Mitigation of nitrogen
436 pollution in vegetated ditches fed by nitrate-rich spring waters. Agriculture, Ecosystems &
437 Environment 243: 74–82.

438 Soana, E., Gavioli, A., Tamburini, E., Fano, E. A. Castaldelli, G., 2018. To mow or not to mow: reed
439 biofilms as denitrification hotspots in drainage canals. Ecol. Eng. 113, 1–10.

440 Tanino, Y., 2012. Flow and mass transport in vegetated surface waters, in: Gualtieri, C., Mihailovic,
441 D.T. (Eds.), Fluid Mechanics of Environmental Interfaces. Second Edition: Taylor & Francis, pp.
442 369–394.

443 Thyssen, N., Erlandsen, M., Jeppesen, E., Ursin, C., 1987. Reaeration of oxygen in shallow,
444 macrophyte rich streams: I–determination of the reaeration rate coefficient. Int. Rev. Hydrobiol.
445 72(4), 405–429.

446 Wanninkhof, R., 1992. Relationship between gas exchange and wind speed over the ocean. J.
447 Geophys. Res. 97, 7373–7381.

448 Weiss, R.F., 1970. The solubility of nitrogen, oxygen and argon in water and seawater. Deep-Sea
449 Research 17(4), 721–735.

450 Wilcock, R.J., Champion, P.D., Nagels, J.W., Croker, G.F., 1999. The influence of aquatic
451 macrophytes on the hydraulic and physico-chemical properties of a New Zealand lowland stream.
452 Hydrobiologia 416, 203–214.

453 Xu, D., Li, Y., Howard, A., Guan, Y., 2013. Effect of earthworm *Eisenia fetida* and wetland plants
454 on nitrification and denitrification potentials in vertical flow constructed wetland. Chemosphere
455 92(2), 201–206.

456 Yager, E.M., Schmeeckle, M.W., 2013. The influence of vegetation on turbulence and bed load
457 transport. J. Geophys. Res.-Earth 118(3), 1585–1601.

458 Zhang, Z., Rengel, Z., Meney, K., 2008. Interactive effects of nitrogen and phosphorus loadings on
459 nutrient removal from simulated wastewater using *Schoenoplectus validus* in wetland microcosms.
460 Chemosphere 72(11), 1823-1828.

461 Zhang, H.Y., Wang, Z.Y., Xu, W.G., Dai, L.M., 2015. Effects of rigid unsubmerged vegetation on
462 flow field structure and turbulent kinetic energy of gradually varied flow. River Res. Appl. 31(9),
463 1166–1175.

Zhang, S., Pang, S., Wang, P., Wang, C., Guo, C., Addo, F.G., Li, Y., 2016. Responses of bacterial community structure and denitrifying bacteria in biofilm to submerged macrophytes and nitrate. Scientific Reports 6, 36178.

469 **Table 1.** Gas transfer velocity of argon (k_{Ar}) measured for vegetated and unvegetated mesocosms in
470 different conditions of water velocity and water temperature (average ± standard deviation, n = 3).
471 The corresponding values normalized to a temperature of 20 °C and a Schmidt number of 600 are
472 also reported (k_{600}).

		k_{Ar} (cm h^{-1})		k_{600} 20 °C (cm h^{-1})	
	Treatment	Vegetated mesocosms	Unvegetated mesocosms	Vegetated mesocosms	Unvegetated mesocosms
Velocity experiment (temperature 16 °C)	0 cm s^{-1}	0.678±0.129	0.669±0.128	0.673±0.128	0.668±0.128
	1.5 cm s^{-1}	3.655±0.477	2.577±0.208	3.507±0.458	2.471±0.201
	3 cm s^{-1}	4.919±0.461	3.205±0.433	4.784±0.445	3.126±0.422
	6 cm s^{-1}	5.452±0.589	3.586±0.353	5.339±0.573	3.534±0.347
Temperature experiment (velocity 3 cm s^{-1})	8.5 °C	3.938±0.277	2.463±0.128	4.701±0.332	2.944±0.156
	16 °C	4.919±0.461	3.205±0.433	4.784±0.445	3.126±0.422
	28 °C	6.458±0.325	4.255±0.236	4.726±0.235	3.127±0.175

473
474

475 **Figure captions**

476 **Fig. 1.** Changes in Ar concentrations in water column mesocosms during the incubations expressed
477 as a natural log-transformed proportion of the initial value (average ± standard deviation, n = 3).
478 Panels A−B and panels C−D report the temporal evolution during the *velocity experiment* and the
479 *temperature experiment*, respectively.

480 **Fig. 2.** Box and Whisker plots of gas transfer velocity (k_{600}) calculated as a function of water velocity
481 and water depth from a set of literature equations (see the text for more details). Experimental values
482 measured in vegetated and unvegetated mesocosms in three conditions of water velocity (average ±
483 standard deviation, n = 3) are also reported. The central horizontal line in the box is the median of the
484 data, the top and bottom of the box are the 25^{th} and 75^{th} percentiles, and the ends of the whiskers are
485 the 10^{th} and 90^{th} percentiles.

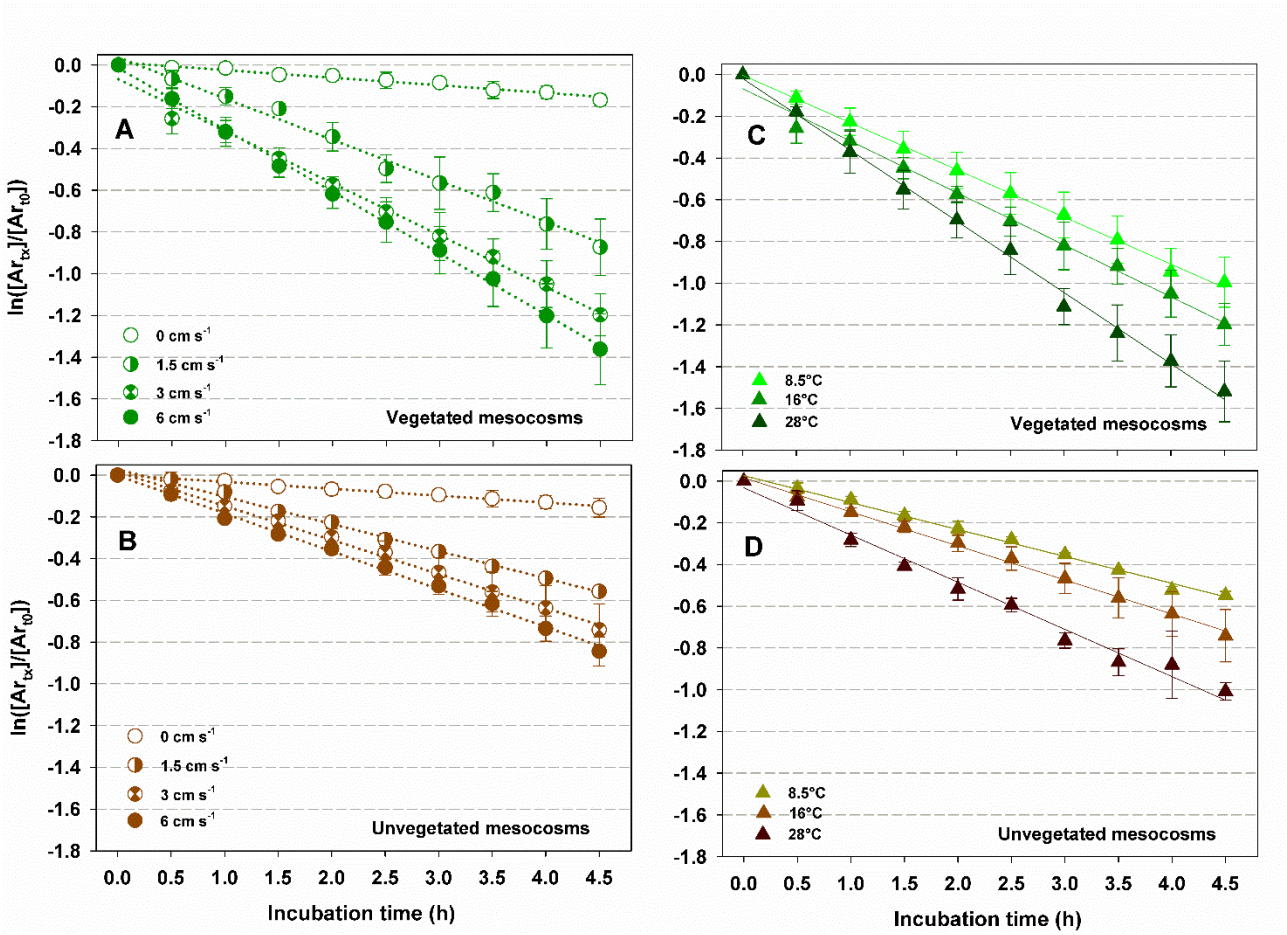
A
B
C
D
0 cm s-1
1.5 cm s-1
3 cm s-1
6 cm s-1
8.5°C
16°C
28°C
Vegetated mesocosms
Unvegetated mesocosms
ln([Art]/[Ar0])
Incubation time (h)

Fig. 1

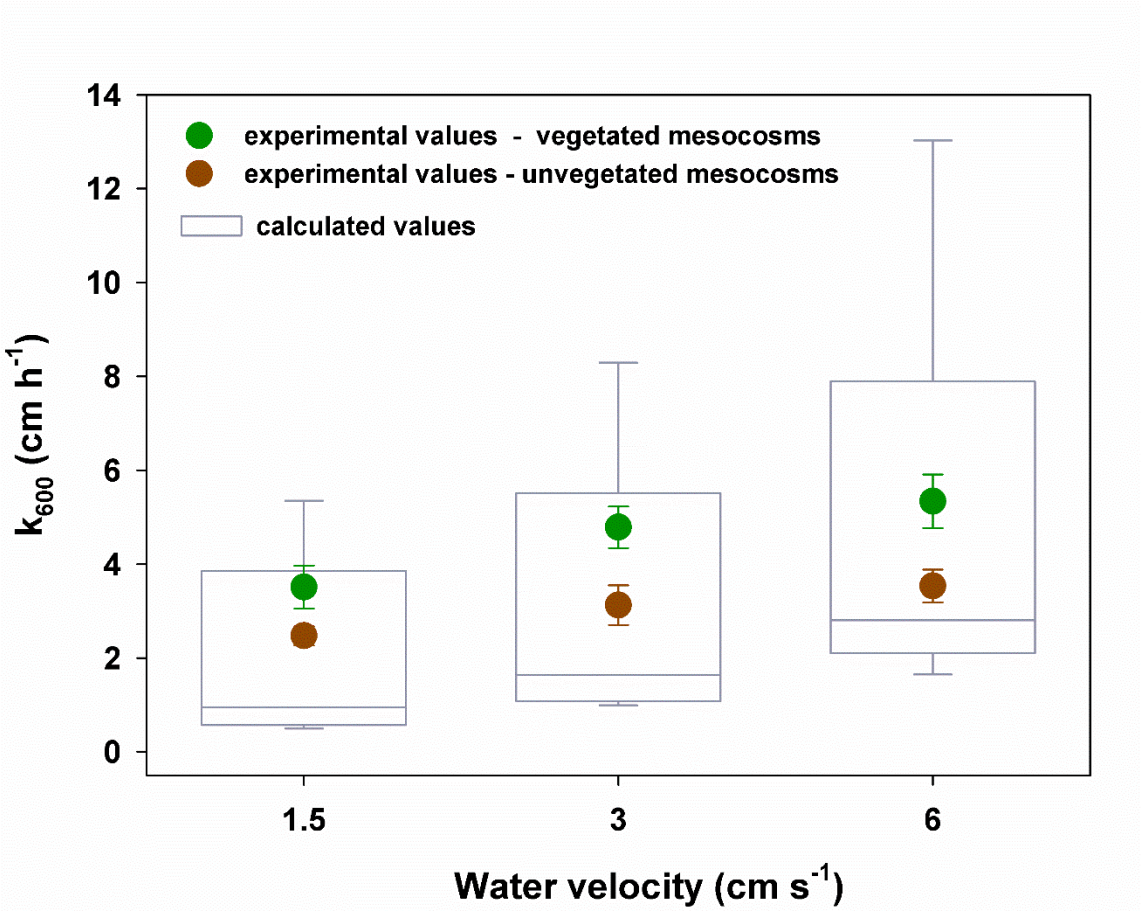
experimental values - vegetated mesocosms
experimental values - unvegetated mesocosms
calculated values
k_{600} (cm h^{-1})
0
2
4
6
8
10
12
14
1.5
3
6
Water velocity (cm s^{-1})

488

489 **Fig. 2**